MG AND SI ISOTOPE FRACTIONATION WITHIN THREE TYPE B CA-AL-RICH INCLUSIONS. K. B. Knight*[,1,2,], N. T. Kita[3], A. M. Davis[1,2,4], F. M. Richter[1,2] and R. A. Mendybaev[1,2], [1]Chicago Center for Cosmochemistry, [2]Department of the Geophysical Sciences, The University of Chicago, Chicago, IL 60637, [3]Department of Geology and Geophysics, University of Wisconsin, Madison, WI 53706, [4]Enrico Fermi Institute, The University of Chicago, Chicago, IL 60637. ♦Present address: Lawrence Livermore National Laboratory, Livermore, California 94550, USA (knight29@llnl.gov).

Introduction: Ca-Al-rich inclusions (CAIs) in CV3 chondrites are the oldest recognized objects formed in the solar system, and provide a unique record of early solar system conditions and processes. Bulk compositions of Type B CAIs from CV3 chondrites show depletions in Mg and, to a lesser degree, in Si, relative to the expectations of equilibrium condensation calculations [1]. These CAIs are also often enriched in the heavy isotopes of Mg and Si by a few ‰ [2,3], a likely consequence of evaporative loss of Mg and Si. While bulk CAIs have isotopically heavy Mg and Si, the isotopic distribution of Si and Mg within individual CAIs remains analytically challenging and incompletely understood. This internal isotopic record may offer additional clues about the conditions of CAI formation, as well as clarification of early solar system processes affecting CAIs prior to incorporation into their host meteorites. In this study, isotopic profiles of Mg and Si were obtained from within three Type B CAIs by secondary ion mass spectrometry (SIMS).

Study Samples: Three Type B CAIs from the CV3 chondrites Allende (USNM-3529.16 and AL-4884) and Leoville (USNM-3535.1) were studied. Previously reported Mg isotope data from melilite in USNM-3529.16 and USNM-3535.1 [4] were recalculated and reexamined, and are included here. To this revised data set, we add new Mg isotopic profiles in melilite from AL-4884, as well detailed Si isotope profiles in melilite from USNM-3535.1 and AL-4884.

Melilite ($Ca_2(MgSi,Al_2)SiO_7$), an abundant mineral in the mantles and interiors of most Type B CAIs, was the primary analytical focus of this study. Melilite in the mantles of Type B CAIs often reflects high-temperature gehlenitic compositions (~$Åk_{25}$) with sharp compositional gradients across distances of a few 100 µm. More åkermanitic compositions (~$Åk_{55-75}$) dominate the interior melilite, which often show normal igneous zoning, with lower-temperature åkermanitic crystal rims and more gehlenitic crystal cores.

For this study we tried to obtain isotopic data over the widest range of melilite compositions possible, with particular focus across the sharp compositional transition present towards the CAI rim. In the CAI interiors, we measured profiles within individual zoned melilite crystals, as well as across a range of melilite compositions and dispersed interior locations.

Methods: Polished CAI sections were characterized using a JEOL JSM-5800LV SEM under high vacuum conditions with a 15 kV accelerating voltage. Quantitative energy-dispersive x-ray (EDX) mapping of sample surfaces enabled generation of melilite Åk content maps, which were used to guide analyses.

Si isotope analyses were obtained using a Cameca IMS-1280 at the University of Wisconsin with a Cs^+ primary beam focused to 10-15 µm. Four Faraday cups were used for simultaneous measurement of ^{28}Si, ^{29}Si, ^{30}Si and ^{27}Al. SIMS-derived isotopic compositions can be affected by matrix composition, with variations in instrumental mass fractionation (IMF) observed as a function of chemical composition. Matrix-appropriate standards are essential to any successful measurement, particularly in the case of Si [5]. The IMF was calibrated using a set of isotopically unfractionated glasses and synthesized zoned melilite to bracket the compositional range of melilite observed in CAIs. Matrix effects can give apparent $\delta^{30}Si$ variations of 6‰ (Fig. 1).

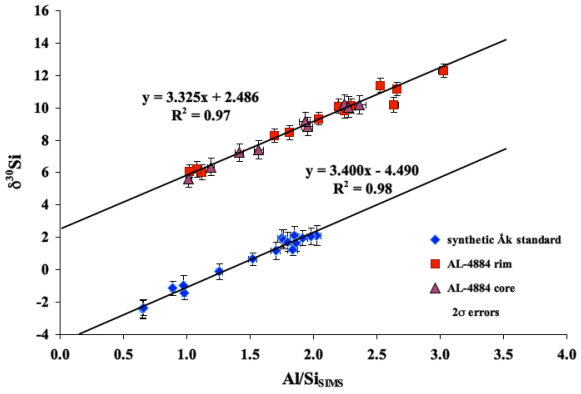

Fig. 1. A comparison of measured $\delta^{30}Si$ in melilite standards and melilite from AL-4884, as a function of composition. The offset is due to AL-4884 containing isotopically heavy Si.

Mg isotope analyses were also obtained using the Wisconsin Cameca IMS-1280, with an O^- primary beam focused to 15–20 µm. Four static Faraday cups enabled simultaneous measurement of ^{24}Mg, ^{25}Mg, ^{26}Mg and ^{27}Al. IMF calibration used the same set of isotopically unfractionated glasses and synthetic melilite.

Measured $^{27}Al/^{24}Mg$ ratios are corrected for relative sensitivity (the difference between the Al/Mg

determined by SIMS and that determined by other techniques such as SEM-EDX or electron microprobe) using the constant relative sensitivity factor, 0.914, as reported by [6]. δ^{25}Mg values are corrected for IMF using the Åk content of the analyzed volume measured as ^{27}Al/^{28}Si, and confirmed by additional SEM measurements. Fractionation-corrected Δ^{26}Mg values are calculated using an exponential law with the slope of 0.514 from the evaporation experiments of [7] and the average Δ^{26}Mg of the standard glasses.

Data acceptance criteria. The Åk content of the analyzed volume and the presence of any other mineral phases in each melilite spot was verified by SEM-EDX, following SIMS analyses. Analytical overlap of multiple mineral phases was a primary source of rejected data. In total, we rejected 2 (of 14) Mg isotopic analyses from USNM-3529.26, none (of 30) from USNM-3535.1, and 13 (of 70) from AL-4884, as well as 9 (of 88) Si isotopic analyses from USNM-3535.1 and 8 (of 32) from AL-4884.

Isotopic Profiles: Although these data were not collected for the purpose of short-lived chronology, all three samples yield scattered but consistent data suggesting agreement with the 'canonical' initial solar system ^{26}Al/^{27}Al ratio of ~4.5×10^{-5}. Mg and Si are isotopically heavy in all samples. Mg becomes isotopically lighter, approaching normal (terrestrial) values towards the rims in all three CAIs studied (Fig. 2), despite the range of interior δ^{25}Mg values. The shift towards lighter δ^{25}Mg values is best correlated with distance (Fig. 2), rather than with Åk content (Fig. 3) in all three CAIs. This behavior is opposite to that reported in [8], where a Type A CAI from Leoville yielded heavier δMg values towards the rim.

Si isotope profiles are nearly flat within AL-4884. Si in USNM-3535.1, however, fractionates in the *opposite* sense of Mg (Fig. 4), becoming isotopically heaviest at the CAI rim. This is similar to Si isotope observations of the Leoville Type A CAI reported by [9].

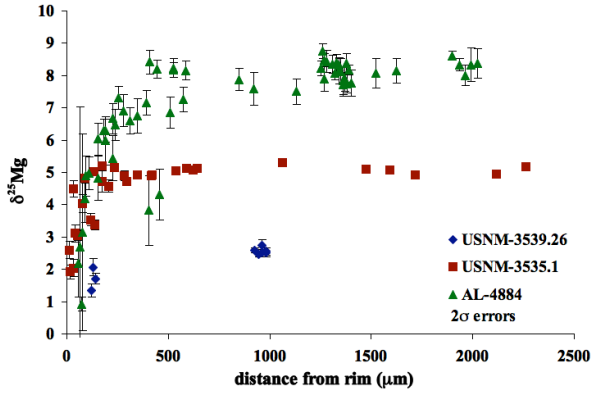

Fig. 2. δ^{25}Mg vs. distance from the rim in melilite from three Type B CAIs.

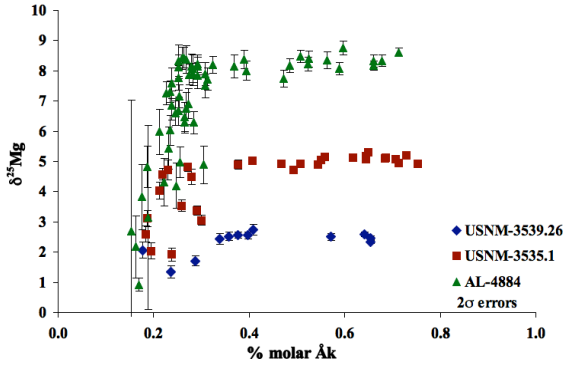

Fig. 3. Melilite δ^{25}Mg vs. mole% Åk in three Type B CAIs.

Discussion: Mg and Si isotope determinations yield contrasting internal fractionation behavior, in marked contrast to the congruent Mg and Si fractionation reported in a Type A Leoville CAI [8,9]. Most puzzling, perhaps, is the isotopically heavy Si rim of USNM-3535.1 suggesting late stage evaporative mass loss, while Mg in the same region of this CAI approaches normal isotopic composition. Post-crystallization and evaporation exchange of Mg with an external reservoir may have occurred, with slow Si diffusion or low Si activity in the external reservoir limiting the exchange of Si. In this scenario, AL-4884 experienced much more evaporative mass loss prior to crystallization, but did not experience a post crystallization evaporation event. It did, however, exchange Mg with an external reservoir, as did USNM-3529.26. Si may preserve late stage evaporation events better than Mg.

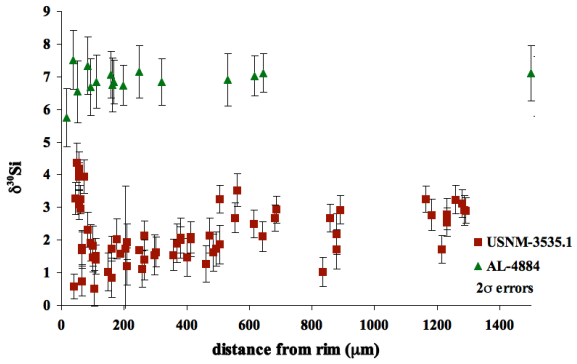

Fig. 4. δ^{30}Si vs. distance from the rim in melilite in two CAIs.

References: [1] Grossman L. et al. (2000) *GCA, 64*, 2879–2894. [2] Clayton R. N. (1988) *Phil. Trans. Royal Soc. Lond., A325*, 483–501. [3] Grossman L. et al. (2008) *GCA, 72*, 3001–3021. [4] Richter F. M. (2007) *LPS XXXVIII,* Abstract #2303. [5] Knight K. B. et al. (in press) *GCA*. [6] Kita N. T. et al. (2007) Workshop on the Chronology of Meteorites and the Early Solar System. [7] Davis A. M. et al. (2005) *LPS XXXVI*, Abstract #2334. [8] Simon J. I. et al. (2005) *EPSL, 238,* 272-283. [9] Shahar A. and Young E. D. (2007) *EPSL, 257*, 497-510.